McNair Scholars Research Journal

Volume 10 Article 13

2017

Determining the Interaction Of Atg11cc2-3 with Its Protein Partners Using In Vitro Binding Assays

Jesse E. Smith
js@emich.edu

DETERMINING THE INTERACTION OF Atg11CC2-3 WITH ITS PROTEIN PARTNERS USING *IN VITRO* BINDING ASSAYS

Jesse E. Smith
Dr. Steven Backues, Mentor

ABSTRACT

Autophagy is a mechanism of cellular upkeep by trafficking intracellular material to be degraded. Autophagy is known to be carried out by autophagy related proteins (Atg), yet the exact mechanism of how autophagy occurs has yet to be discovered. Due to its clinical relevance to conditions such as neurodegenerative and muscular diseases, a great deal of current research is being dedicated to further our understanding of how autophagy occurs. Atg11, a protein critical to a yeast's ability to perform selective autophagy, may also hold many answers to selective autophagy within humans. Atg11 is a coiled-coil protein that interacts with Atg1, 9, 11, 20, 29, along with Ypt1 in selective autophagy. However, it is unknown how these interactions occur. Does Atg11 have multiple binding sites where it may bind to proteins simultaneously? Or does Atg11 have one competitive binding site where it can only bind with a single protein, and then release it before it may bind again? In this research we attempt to purify the binding portion of Atg11 so that it can be used to observe Atg11's binding interactions with these proteins through a protein binding test mediated by a resin pulldown.

INTRODUCTION

Neurodegenerative diseases in humans fall beyond the reach of most current means of pharmaceutical interventions.

With advancements in treatments for cancer and cardiovascular diseases, the life expectancy of many individuals is expected to increase (1). An increase in life expectancy may also increase the likelihood of developing a neurodegenerative disease. As one's age and life expectancy increases, the amount of years their neurons and muscle cells (myofibrils) have been in existence increases, as well. This is because neurons and myofibrils lack the ability to undergo cell division (2). With cellular division being the primary means for the regeneration of tissues, non-dividing cells must possess a different means to aid in their survival over the course of one's lifespan.

Longevity in nervous and muscle tissue is thought to be correlated to a cell's ability to maintain proper function. In nervous and muscle tissue, to maintain proper function, a large sum of energy produced from the mitochondria is required. A buildup of waste and free radicals that damage cellular structures is more likely because of mitochondrial activity (3). Lysosomal degradation compensates for this by aiding in the degradation and recycling of damaged cellular material (4).

Macroautophagy (referred to as "autophagy") is a process that aids the lysosome in cleaning up these damaged cell structures (5). Autophagy describes an intracellular process in which material is wrapped in a double membrane vesicle, known as an autophagosome (**Figure 1**), and transported for degradation in either a lysosome (in animals), or vacuole (in other eukaryotes) (6). The two primary categories of autophagy describe the intracellular content being packaged for degradation.

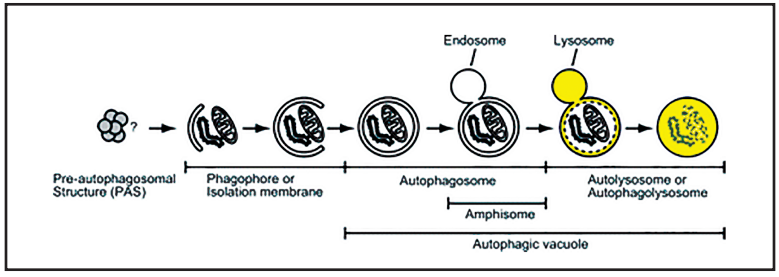

Figure 1: *General depiction of autophagy within mammalian cells.* Autophagy is process in which intracellular material is wrapped into a double membrane vesicle known as an autophagosome and transported to be degraded. (Figure adapted from reference 8).

Bulk autophagy describes an intracellular response to starvation in which a large amount of non-specific material is packaged and sent for degradation. In contrast, selective autophagy describes a process in which a specific cargo is recognized as needing to be degraded (7). Though both forms of autophagy are vital for cellular survival, selective autophagy attracts attention from researchers due to its implications for neurodegenerative diseases.

Further delineation of selective autophagy has occurred through these investigations. Selective autophagy may be categorized in regards to the size of its payload to be degraded (7). Additional classifications of selective autophagy are made by describing the actual content being transported (9). Through xenophagy eliminating pathogenic structures within a cell, aggrephagy eliminating denatured polyubiquitinated proteins, mitophagy eliminating damaged mitochondria, and lipophagy specifically targeting lipids for degradation, no cellular content seems to fall outside of the reach of autophagy. For this reason, a dysfunction in the cell's ability to perform autophagy may lead to a buildup of dysfunctional intracellular content.

A cell's ability to perform autophagy effectively has been found to both aid and hinder a diseased individual, depending on the situation (4)(10)(11)(12)(13). Autophagy possesses a multi-faceted role in cancer. In breast, prostate, and ovarian cancer victims, disruption of an autophagy regulatory complex known as monoallelic Beclin 1 on chromosome 17q21 has been found in 40 to 75% of patients (11). Additionally, a cell that lacks in the ability to perform mitophagy may experience a buildup of metabolic waste due to mitochondrial dysfunction, which puts additional stressors on DNA, increasing the chance of damage (14). Once cancer tumors develop, the ability to perform autophagy may increase the likelihood of survival for a tumor in times of nutrient deprivation(12).

In neurodegenerative diseases, mitochondrial dysfunction and an accumulation of protein aggregates are two aspects of pathogenesis that can be prevented by autophagy (15)(16). An accumulation of dysfunctional proteins with polyglutamine rich protein extensions blocks certain autophagy pathways, rendering a

cellular response to this protein build up impossible (9). Additional buildup of proteins that interfere with autophagic pathways and lysosome function progress the development of both Huntington's and Alzheimer's disease (16)(18). Pharmaceutical intervention to induce autophagy aids in treating these diseases' pathogenesis. However, there are limited options (14)(17).

Autophagy related proteins (Atg) are thought to provide the answer to many of these questions regarding the buildup of cellular debris (1). Atg proteins, along with additional factors, are known to induce autophagy. There are over 35 known Atg proteins, half of which are vital to autophagy. Based on their function, certain Atg proteins are categorized as necessary for bulk or selective autophagy. Of these Atg proteins, Atg11's role in selective autophagy will be the focus of this research. Atg11 in yeast functions as a scaffolding protein that aids in the production of the autophagosome assembly site. Atg11 does this by binding to a variety of partners, including Atg17, Atg9, and Atg1 (**Figure 2**), in addition to cargo receptors allowing for the autophagosome to be formed (18)(19). It is known that the coiled coil domains two through three (CC2-3) are required for Atg11's self-interaction, along with its interactions with Atg1 (19). The extent of these

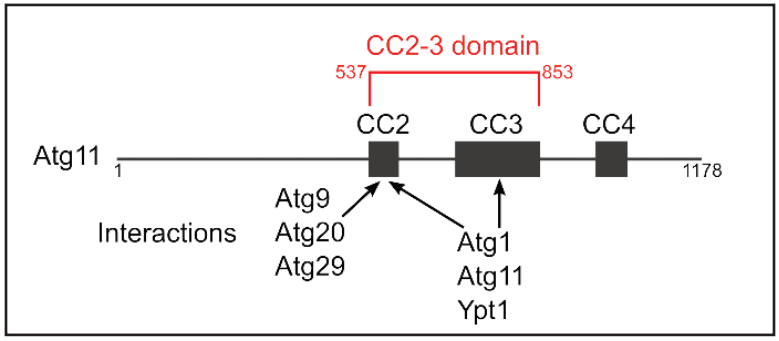

Figure 2: *Atg11's interactions by coil-coiled domain:* This diagram shows the interactions of Atg11 through its coiled-coil domains 2-3. Figure courtesy Dr. Steven Backues.

interactions, however, is not understood.

This study will aid in further understanding of Atg11 in yeast, which in turn will aid in understanding autophagy related proteins in humans. By furthering the understanding of Atg11's

role within selective autophagy in yeast, it is hoped that the role of its homologs (Huntingtin and FIP200) can be further understood within humans (20). The goal of this research is to gain insight in Atg11's scaffolding ability. Does Atg11 bind to multiple partners at once? Or, is Atg11 limited to one binding site in which inhibition may occur between other Atg partners?

RESULTS

In an effort to use ligase independent cloning to produce an expression clone of ATG11 CC2-3, a Polymerase Chain Reaction was performed (PCR). The goal of our PCR was to amplify the ATG11 CC2-3 region. The region amplified in the PCR is from base pair 961 to 2577, corresponding to amino

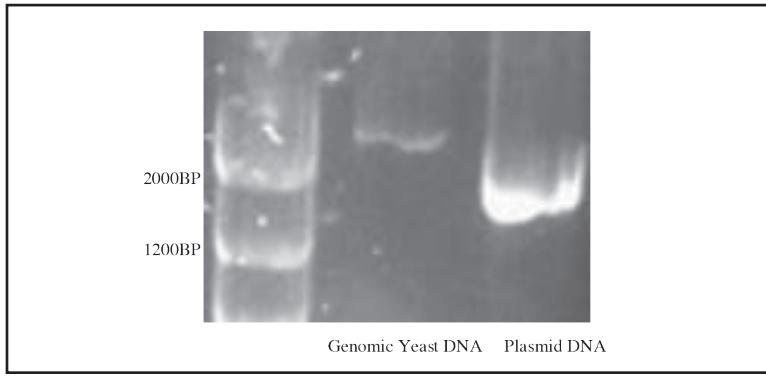

Figure 3: *ATG11CC2-3b inserts amplified from genomic yeast DNA (lane 2) and recombinant plasmid DNA (lane 3)*. Through PCR amplification using genomic yeast and plasmid DNA, the ATG11CC2-3b gene was amplified (amino acids 321-859 corresponding to roughly 1600 base pairs). Plasmid DNA yielded a large band at 1600 base pairs, as visualized by DNA electrophoresis.

acids 321-859 on Atg11, previously reported to correspond to the CC2-3 region by Lippotova (8). One template was genomic yeast DNA (fryf43sas2Δ) and the other template was a plasmid containing ATG11 (pRS414-ATG11-19-23-27). The completed PCR reactions were separated on a 2% agarose gel (**Figure 3**). Plasmid pRs414-ATG11-19-23-27 yielded an intense band at around 1600bp, which is the expected size for ATG11CC2-3b. For this reason, this PCR product was selected as the insert for the ligation independent cloning (**Figure 3**).

Following PCR, the selected PCR product was purified using a PCR purification kit, and the concentration of the purified DNA was found to be 270ng/ul. T4 treatment of the DNA was then performed; the goal of this was to eliminate flanking base pairs to prepare the "sticky" ends of the DNA so it could be inserted into the pMCSG10 *E. coli* vector. To complete the ligation independent cloning, the T4 treated insert was then annealed with the linearized, T4 treated pMCSG10 vector and transformed into DH5α competent cells. Four colonies were picked from the plate, and the DNA was purified by a miniprep procedure. To determine which of the selected colonies contained the desired insert, each of the four DNA clones isolated by miniprep was amplified by PCR using primers recognizing ATG11CC2-3b, and the PCR products were separate on a 2% agarose gel (**Figure 4**). Since bands from all four clones were seen at around 2000bp, each clone was sequenced.

Unfortunately, analysis of the sequencing results revealed a frameshift mutation in all of the samples, which could be traced back to an error in the design of the primers initially used to

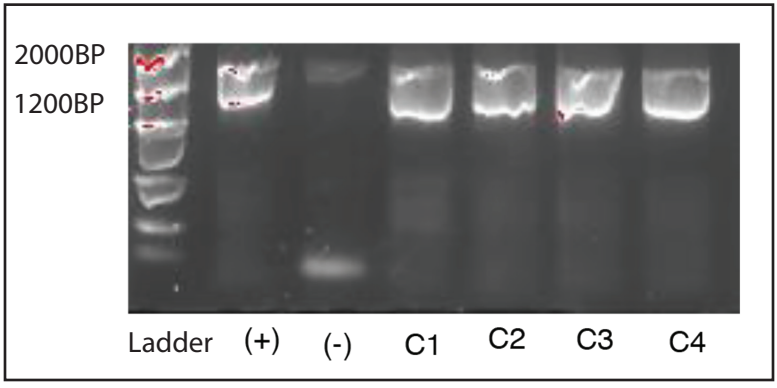

Figure 4: *pMCSG10-ATG11CC2-3 present in transformed E. coli.* A 2% gel was run of a PCR of 4 transformed colonies (C1-4) checking for the presence of ATG11CC2-3b in pMCSG10. The positive control (+) was another plasmid that also contained this region, pMCSG10-Atg11CC2-3a while the negative control (-) was an empty pMCSG10 vector. It was found that ATG11CC2-3b was present in all four clones.

amplify the ATG11CC2-3b insert (**Figure 5**).

Therefore, the initial PCR amplification was repeated using the same template but with corrected primers. The PCR

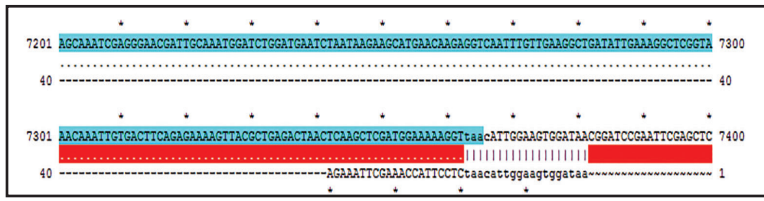

Figure 5: *Primer error for ATG11CC2-3b.* Showing the error in primer 226 (bottom strand) compared to our pMCSG10-ATG11CC2-3b design (top strand). The primer includes 20 base pairs out of frame starting at base pair 7380 of the ATG11 gene. Since 20 is not a multiple of 3, this led to a frameshift mutation that added an additional 33 erroneous amino acids before a stop codon was reached.

products were run on a 2% gel following the amplification of ATG11CC2-3b using the new primers (**Figure 6**).

As one may see, at 1600bp in lane two there is a band leading one to believe that the desired ATG11CC2-3b fragment

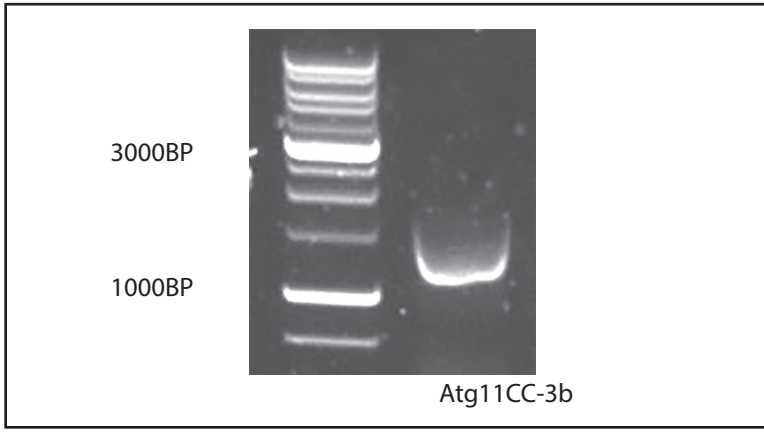

Figure 6: *Atg11CC2-3b amplified via PCR using new primers* ATG11CC2-3b was amplified by PCR using new primers, and the product and checked on a 2% agarose gel versus a standard 1KB ladder.

was produced. A PCR purification procedure was performed on this DNA, yielding a concentration of 33 ng/ul, followed by T4 treatment of this DNA, and then annealing it to pMCSG10 and transforming the plasmid into DH5alpha cells. Following the transformation, three colonies were selected and the DNA isolated by miniprep. The presence of the insert was verified by PCR with primers recognizing ATG11CC2-3b, and the products were

separated via a 1% agarose gel (**Figure 7**).

ATG11CC2-3b appeared to be present in all three clones, so they were sent for sequencing. Positive sequencing results

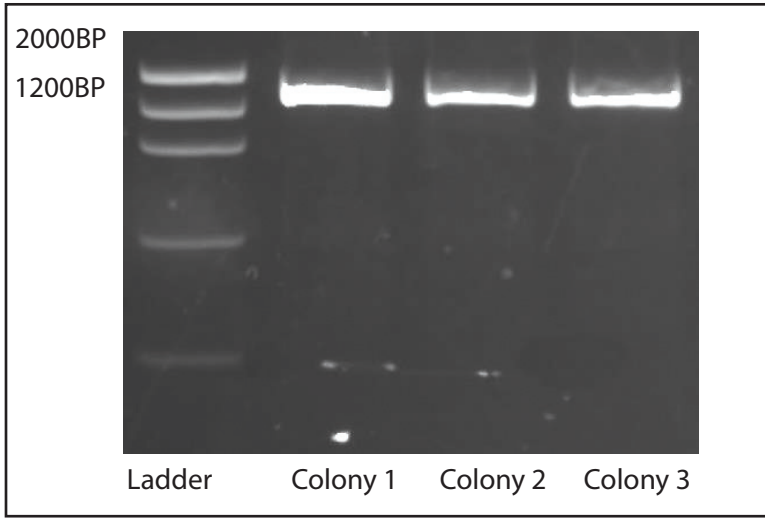

Figure 7: *pMCSG10-ATG11CC2-3b expressed in E. coli.* A 2% gel of a PCR checking for ATG11CC2-3b in each of three putative clones of pMCSG10-ATG11CC2-3b, each isolated from an individual transformed colony . Each colony appeared to have a band at roughly 1600 base pairs representing ATG11CC2-3b.

demonstrated that pMCSG10-ATG11CC2-3b had been successfully created with no frameshift mutations or other errors (**Figure 8**).

A sample of pMCSG10-ATG11CC2-3b DNA was transformed into Rosetta competent cells, with the goal of

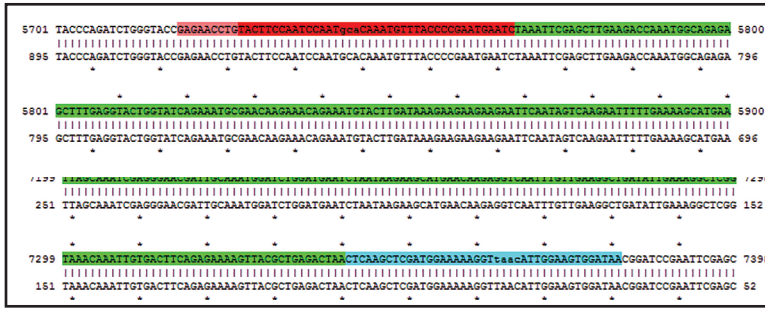

Figure 8: *Sequencing Results using the new primers.* Analysis of cloning sequencing results using primers 221 (binding region highlighted in red representing the forward sequence) and 246 (binding region highlighted in light blue representing the reverse sequence Sequencing results confirmed presence of base pairs 961 to 2577 of Atg11, which code for the CC2-3b region.

producing as much purified Atg11CC2-3b protein as possible. The Rosetta cells were induced overnight via auto induction and lysed via sonication. Following lysis, the content of the cells was separated into soluble, insoluble, and glutathione resin-bound fractions. The glutathione-S transferase (GST) is encoded in the pMCSG10 vector, so that the Atg11CC2-3 protein is produced with GST attached, thereby allowing the protein to bind to the glutathione resin. Following lysis and fractionation, a 12.5% SDS

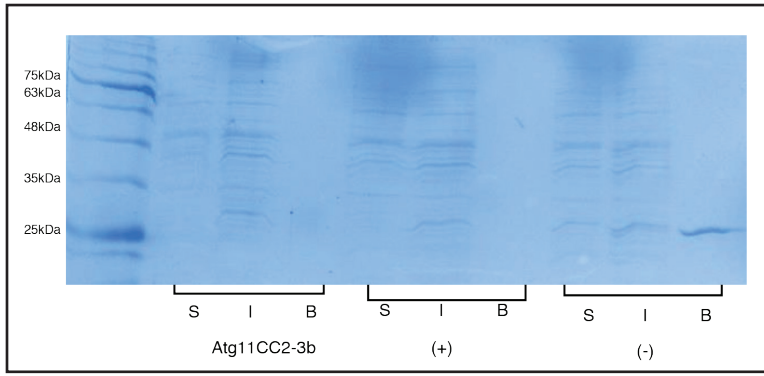

Figure 9: *Atg11CC2-3b does not express well in E. coli.* pMCSG10-Atg11CC2-3b was transformed into Rosetta cells and induced through autoinduction to express Atg11CC2-3b. The cells were lysed and separated into soluble (S), insoluble (I), and glutathione resin bound (B) fractions and samples were run on a 12.5% SDS page gel. The positive control was a previously produced version of Atg11CC2-3a (+), while the negative control was pMCSG10-empty. No band corresponding to Atg11CC2-3b could be seen, suggesting that it does not express at sufficient levels.

page gel of the soluble, insoluble, and resin bound fraction of the cells proteins was run.

The negative control is the GST alone from the empty pMCSG10 vector. The negative control bound sample has a band in the right region for GST, indicating that autoinduction worked, and the resin binding was effective. The positive control, however, did not produce a band within the GST bound lane, indicating expression of Atg11CC2-3a did not occur. In addition, it appears that the cell lysis is not occurring as effectively as we would like, due to the fact that the soluble lane does not contain as much material as it would if all the cells were to lyse.

DISCUSSION

Sequencing results confirmed the successful creation of pMCSG10-ATG11CC2-3b within our strains of *E. coli.* However, since Atg11CC2-3b protein was not seen in a small scale resin binding test, our protocol for protein expression proved to be inadequate. Similar projects were done in our laboratory using various ATG11 constructs, with pMCSG10-ATG11CC2-3a being the only construct found to express Atg11. Other expression projects in our laboratory centered on Atg11, including the project discussed in this paper, have all failed to produce Atg11 at adequate concentration, purity, and stability to test for protein interactions using biochemical means. The failure to express and purify Atg11CC2-3b in *E. coli* has led our laboratory to rethink our methods. Moving forward, we as a laboratory are transitioning to using a yeast two hybrid assay to test for interactions of Atg11 and its binding partners. This is an established approach that does not require the expression and purification of any proteins, but instead uses various autophagy related proteins attached to a DNA binding domain within yeast, and various ATG11 constructs attached to an activating domain.

METHODS

Vector selection:

The expression vector pMCSG10 was created by the Midwest Center for Structural Genomics and was a gift of Dr. Hana Popelka (Laboratory of Dr. Daniel Klionsky, University of Michigan) (22). Its key features area T7 promoter, an N-terminal Glutathione-S-Transferase (GST) tag, and a Ligation Indpendent Cloning (LIC) compatible multiple cloning site.

Atg11 Insert Production by PCR:

Primers were designed to produce an ATG11CC2-3b insert (base pairs 961-2577 of the Atg11 coding sequence) through ligation independent cloning (**Table 1**). Primers SKB221 and SKB226 were used for insert produced in **Figure 3** and checked in **Figure 4**, while SKB221 and SKB246 were used for the insert in **Figure 5** and checked in **Figure 7**. DNA to be amplified was supplied by *E. coli* plasmid pRS414-ATG11-19-23-27. The PCR

was performed using Phusion DNA polymerase (New England Biolabs) according to manufacturer's protocol.

Primer Name	Primer Function	Primer Sequence
SKB221	Forwards primer for LIC cloning of ATG11CC2 (a.a. 321)	tac ttc caa tcc aat gca CAA ATG TTT ACC CCG AAT GAA TC
SKB226	Incorrect reverse primer for LIC cloning of ATG11CC3 (a.a. 859)	ttatccacttccaatgtta GAGGAATGGTTTCGAATTTCTCA
SKB246	Corrected Reverse primer for LIC cloning of ATG11CC3 (a.a. 859)	ttatccacttccaatgttaACCTTTTT CCATCGAGCTTGAG

Table 1: *Primers used for PCR amplification of Atg11CC2-3b:*

DNA Gel Electrophoresis:

Electrophoresis was performed at 120V using TAE buffer and an agarose gel. 1% gels were made using 50mL of buffer, 0.5g of agarose (1g in 2% gels), and 1.5ul of Gel Red (Biotium). Gels were imaged with a BioRad ChemiDoc XRS+ Molecular Imager using the manufacturer's protocol.

T4 Treatment:

T4 processing was used to eliminate bases at the end of both our insert (ATG11CC2-3b) and vector (pMCSG10) to create overlap between the two strands. T4 DNA Polymerase was purchased from ThermoFisher. The T4 treatment consisted of a PCR cycle consisting of 35 minutes at 22°C, 20 minutes at 75°C, and then cooling on ice. The reaction mixture for the T4 treatment of pMCSG10 included 5ul of linearized plasmid, 12ul of 5x buffer, 3ul of 100mM DTT, 2.5ul of 100mM dGTP, 1.5ul of T4 DNA polymerase, and 35ul of dH20. The reaction mixture for the T4 reaction of Atg11CC2-3b included 5ul of insert, 12ul of 5x buffer, 3ul of 100mM DTT, 2.5ul of 100mM dCTP, 1.5ul of T4 DNA polymerase, and 35ul of dH20.

Insert Annealing to Vector:

Annealing of the ATG11CC2-3b to pMCSG10 occurred by mixing 1ul of T4-treated plasmid with 2ul of T4-treated insert, incubating for 10 minutes at 22°C, adding 1ul of 25mM EDTA, incubating for five minutes at 22°C, and then holding on ice until ready for use.

Transformation into *E. coli* cells

Transformation of the annealed construct into *E. coli* DH5α cells started with thawing 100ul of competent cells on ice for five minutes, adding 1ul of DNA, incubating for 30 minutes on ice, heat shocking for 42 seconds at 42°C, incubating on ice for two minutes, and then suspending in 1mL of SOB and incubating with rotation at 37°C for an hour. 100ul of mixture was spread on one plate (10% plate), while the other 900ul was pelleted via centrifugation at 13,000 RPM in a Sorvall Biofuge Pico and resuspended in 100ul of SOB then plated (90% plate). Plates were incubated for 24 hours at 37°C.

Small Scale Resin Binding Test:

Autoinduction was used to induce *E. coli* containing the construct into producing Atg11CC2-3b (21). Autoinduction occurred in autoinduction media containing 1% tryptone, 0.5% yeast extract, 25 mM Na_2HPO_4, 25 mM KH_2PO_4, 50 mM NH_4Cl, 5mM Na_2SO_4, 0.5% glycerol, 0.2% α-lactose, 0.05% glucose, and 2 mM $MgSO_4$. The autoinduction media was prepared with carbenicillin (50ug/ml) and chloramphenicol (34ug/ml) and inoculated. The cultures were grown overnight, harvested by centrifugation at 12,000g for 1 minute, washed with a solution of 25mM HEPES pH 7, 150mM NaCl, and 5% glycerol (known as PEB1), and re-suspended in 1ml PEB1 with 10mM β–ME and 1mM PMSF. The cells were lysed via sonication at three ten second pulses at a power level of 4 with 30 seconds cooling on ice between pulses. Fifty (50)ul of 20% TX-100 detergent were added to the mixture and the mixture was vortexed. Samples were then centrifuged for 10 minutes at 10,000g and 4°C. The supernatant (soluble fraction) was removed and saved for further processing. The pellet was then suspended in 200ul of 2xSSB (insoluble fraction). Twenty-five percent (25%) glutathione resin in PEB1 was added to the supernatant to bind with the GST tag (bound fraction). This solution was mixed for 30 minutes at 4°C, then the resin was isolated by centrifugation at 300g for 1 minute at 4°C, washed three times with PEB1+1% TX-100+10mM β-ME+1mM PMSF, re-suspended by inversion and washed with PEB1+10mM β-ME+1mM PMSF. The buffer was removed and 25ul of 2xSSB

was added. Samples of the soluble and insoluble fractions for SDS-page analysis were prepared by combining 20ul of each fraction with 20ul of 2xSSB. SDS page gels (12.5%) were run at 120V, stained with Coomassie Blue, and imaged in a BioRad ChemiDoc XRS+ Molecular Imager.

REFERENCES

Mathers, C. D., Stevens, G. A., Boerma, T., White, R. A., & Tobias, M. I. (2015). Causes of international increases in older age life expectancy. *The Lancet*, *385*(9967), 540-548.

Goedert M, Clavaguera F, Tolnay M. (2010). The propagation of prion-like protein inclusions in neurodegenerative diseases. *Trends Neurosci* 33:317-25.

Ravikumar B, Sarkar S, Davies J.E. (2010). Regulation of mammalian autophagy in physiology and pathophysiology. *Physiol Rev 90*, 1383-435.

Dehay, B., Martinez-Vicente, M., Caldwell, G. A., Caldwell, K. A., Yue, Z., Cookson, M. R. & Bezard, E. (2013). Lysosomal impairment in Parkinson's disease. *Movement Disorders*, *28*(6), 725-732.

Kamber, Roarke A., Christopher J. Shoemaker, & Vladimir Denic. (2015). "Receptor-bound targets of selective autophagy use a scaffold protein to activate the Atg1 kinase. *Molecular Cell 59*(3), 372-381.

Jiang, X., Overholtzer, M., & Thompson, C. B. (2015). Autophagy in cellular metabolism and cancer. *Journal of Clinical Investigation*, *125*(1), 47.

Backues, S. K., & Klionsky, D. J. (2012). Atg11: a Rab-dependent, coiled-coil membrane protein that acts as a tether for autophagy. *Autophagy*, *8*(8), 1275-1278.

Mizushima, N. (2007). Autophagy: process and function. *Genes & Development*, *21*(22), 2861-2873.

Choi, A. M., Ryter, S. W., & Levine, B. (2013). Autophagy in human health and disease. *New England Journal of Medicine*, *368*(7), 651-662.

Gao X, Zacharek A, Salkowski A, et al. (1995). Loss of heterozygosity of the BRCA1 and other loci on chromosome 17q in human prostate cancer. *Cancer Res 55*, 1002-5.

Liang XH, Jackson S, Seaman M, et al. (1999). Induction of autophagy and inhibition of tumorigenesis by beclin 1. *Nature 402*, 672-676.

Rubinsztein DC, Codogno P, Levine B. (2012). Autophagy modulation as a potential therapeutic target for diverse diseases. *Nat Rev Drug Discov 11*, 709-30.

Saito H, Inazawa J, Saito S, et al. (1993). Detailed deletion mapping of chromosome 17q in ovarian and breast cancers: 2-cM region on 17q21.3 often and commonly deleted in tumors. *Cancer Res* 53: 3382-5.

White E. (2012). Deconvoluting the context dependent role for autophagy in cancer. *Nat Rev Cancer 12*, 401-10.

Jellinger KA. (2010) Basic mechanisms of neurodegeneration: a critical update. *J Cell Mol Med 14*, 457-87.

Imarisio S, Carmichael J, Korolchuk V, et al. (2008). Huntington's disease: from pathology and genetics to potential therapies. *Biochem J* 412:191-209.

Geisler S, Holmström KM, Skujat D, et al. (2010). PINK1/Parkin-mediated mitophagy is dependent on VDAC1 and p62/SQSTM1. *Nat Cell Biol 12*, 119-31.

Yorimitsu, T., & Klionsky, D. J. (2005). Atg11 links cargo to the vesicle-forming machinery in the cytoplasm to vacuole targeting pathway. *Molecular Biology of the Cell*, *16*(4), 1593-1605.

He, C., Song, H., Yorimitsu, T., Monastyrska, I., Yen, W. L., Legakis, J. E., & Klionsky, D. J. (2006). Recruitment of Atg9 to the preautophagosomal structure by Atg11 is essential for selective autophagy in budding yeast. *J Cell Biol*, *175*(6), 925-935.

Ochaba, J., Lukacsovich, T., Csikos, G., Zheng, S., Margulis, J., Salazar, L., & Saudou, F. (2014). Potential function for the Huntingtin protein as a scaffold for selective autophagy. *Proceedings of the National Academy of Sciences,* 111(47), 16889-16894.

Eschenfeldt, W. H., Lucy, S., Millard, C. S., Joachimiak, A., & Mark, I. D. (2009). A family of LIC vectors for high-throughput cloning and purification of proteins. *High Throughput Protein Expression and Purification: Methods and Protocols*, 105-115.

Studier, F. W. (2005). Protein production by auto-induction in high-density shaking cultures. *Protein expression and purification*, *41*(1), 207-234.